$Gd_{0.05}Bi_{0.15}M_{0.05}Ce_{0.75}O_2$ solid solutions for IT-SOFC electrolyte application

I. V. Zagaynov[†], S. V. Fedorov

[†]igorscience@gmail.com

A. A. Baikov Institute of Metallurgy and Material Science RAS, 49 Leninsky Av., Moscow, 119331, Russia

A large part of the world's energy demand is met by fossil fuels. Fossil fuels are limited sources and they cause environmental pollution. Among the alternative energy sources, solid oxide fuel cells (SOFCs) attract attention. Ceria doped with heterovalent cations, such as rare earth and alkaline earth ions, have been extensively studied as the most promising electrolyte materials for intermediate temperature solid oxide fuel cells (IT-SOFC). As well known, phase purity and relative density are important factors for obtaining high performance doped ceria electrolytes. The nanocrystalline powders of Gd-Bi-M-Ce-O (M = Cu, Zr, Ni, Co, Mn) solid solutions with the size of about 10 nm were used as precursors to ceramics formation, sintered at 750°C in air, for the application of these materials as a perspective electrolyte for IT-SOFC. Crystal structures and morphologies of these products were characterized by X-ray diffraction (XRD) and scanning electron microscopy (SEM) techniques. The electrical conductivity was measured by AC impedance spectroscopy in the temperature range of 450 – 750°C in air. It was showed that $Gd_{0.05}Bi_{0.15}Mn_{0.05}Ce_{0.75}O_2$ ceramics is the perspective electrolyte and has the conductivity of $8 \cdot 10^{-3}$ S/cm. Ceria doped with these oxides have a high ionic conductivity by the formation of oxygen ion vacancy due to the substitution of Ce^{4+} with other cations.

Keywords: ceria, solid solution, electrolyte, IT-SOFC.

1. Introduction

Solid electrolyte CeO_2 doped with Gd_2O_3 (GDC) is of great interest in the use in intermediate temperature solid oxide fuel cells (SOFC), operated at 500 – 750°C, due to its high conductivity, which is several times higher than the conductivity of YSZ electrolyte. In addition, GDC is chemically compatible with highly active cathode materials based on cobaltites and ferrocobaltites, and its thermal expansion coefficient (CTE) is close to CTE of electrodes [1 – 3]. Doped ceria is considered to be a promising electrolyte and it was demonstrated that the maximum ionic conductivity occurred at 20 mol.% doped systems.

It is shown that the introduction of additives in the amount of 1 – 5 mol.% significantly increases the rate of shrinkage and reduces the sintering temperature up to 800 – 1100°C [4, 5]. The development of more stable electrolytes based on GDC and bismuth oxide, using as a sintering additive without preservation of bismuth oxide [6 – 9] or a second dopant with the preservation of the initial composition of the solid solution based on ceria [10], is proposed. Moreover, triple-doping or multi-doping in ceria has been studied and succeeded to improve the ionic conductivity of ceria [11 – 13]. However, further investigations are still required on tri- or multi-doped ceria in order to develop new electrolytes for future SOFC applications. Thus, it is necessary to investigate ceramics, based on ceria solid solution with three dopants $Gd_{0.05}Bi_{0.15}M_{0.05}Ce_{0.75}O_2$ (M = Cu, Zr, Ni, Co, Mn) as a promising electrolyte for IT-SOFC, which was carried out in this work.

2. Material and methods

$Ce(NO_3)_3 \cdot 6H_2O$, $Bi(NO_3)_3 \cdot 5H_2O$, $Gd(NO_3)_3 \cdot 6H_2O$ and $Cu(NO_3)_2 \cdot 3H_2O$ or $ZrO(NO_3)_2 \cdot 7H_2O$ or $Ni(NO_3)_2 \cdot 6H_2O$ or $Co(NO_3)_2 \cdot 6H_2O$ or $Mn(NO_3)_2 \cdot 4H_2O$ (Acros Organics) were used as initial salts. Appropriate amounts of salts were dissolved in concentrated nitric acid (68%) with the concentration of salts of 0.667 M. After the dissolution of salts, this mixture was added to distilled water, giving the concentration of 0.1 M and after stirring acetylacetone (Hacac) was added (Hacac/Σ(Me) = 1). Then, the co-precipitation was carried out by addition of 2.5 M KOH solution up to pH 11. Ultrasonic processing (35 kHz, 150 W) was used throughout the process at 30°C under stirring. The resulting precipitates were filtered, washed with distilled water-ethanol solution (H_2O/C_2H_5OH = 9 vol.), dried at 150°C for 12 h, and calcined in static air by heating at a rate of 4°C/min from room temperature to 500°C and kept at 500°C for 1 h in a muffle furnace.

The as-obtained powders were pressed into pellets (with 10 wt.% binder made of 5% aqueous solution of polyvinyl alcohol) with 10 mm in diameter and 1 mm in thickness at 150 MPa. Then they were sintered at 750°C (T_{sint}) for 4 h in air with heating of 4°C/min. To fabricate symmetric cells for the impedance studies (Elins Z-350M impedance meter, the frequency range from 0.1 Hz to 1 MHz at an amplitude of AC signal of 30 mV), platinum paste was brushed onto both sides of the electrolyte pellets, and were dried at 150°C for 1 h and annealed at 750°C for 4 h in air. Platinum wires were used as current conductors.

All powders and ceramics were characterized by XRD (DRON-3M, $Cu_{K\alpha}$ radiation), SEM (TESCAN VEGA II SBU with INCA Energy 300 energy dispersive spectrometers), microscopy (Olympus Lext OLS3000 confocal scanning laser microscope), TG-DSC (Netzsch STA449F3, 10°C/min in air), microhardness test (Struers Duramin-5). The relative density of ceramics was determined by hydrostatic weighing.

3. Results and Discussion

The XRD pattern of calcined powders at 500°C (Fig. 1a) shows that the only single phase of the solid solution was formed, and no peaks of other phases were detected. When the spectrum is completely approximated, it is determined that it is also possible to form an amorphous copper oxide and cobalt oxide in the corresponding samples (rather in the form of very small particles), which can form on the surface of the solid solution connected to the subsurface layers of the lattice, where they are enriched with the corresponding cations (these particles grow as a continuation of the surface). All peaks show the typical fluorite structure of ceria (Fm3m). The unit cell parameter changes with adding a third dopant (Table 1). Sample 2 has a lower lattice parameter, which may be related to greater homogeneity with adding zirconium as it often occurs. The average crystallite size calculated using the Scherrer formula was about 8–12 nm and slightly increased in the presence of a third component, except for sample 5. The stability of solid solutions was estimated by TG-DSC. The peaks at 750–800°C can be attributed to the formation of other phases and at >1000°C with the evaporating process of Bi compounds [10,14]. XRD pattern of the calcined powders at 1000°C (Fig. 1b) shows that both phase of ceria solid solution and other phases were formed. In all samples, there is a phase of Bi_2O_3 (γ-Bi_2O_3, sillenite, cI66), which was not found in the system without a third dopant [14]. The formation of other phases was observed (Bi_2CuO_4 in sample 1; the composition of the sillenite varies in the broadest range of $Bi_{13}O_{20}$ – $Bi_5Co_8O_{20}$ in sample 4; $GdMn_2O_5$ phase (oP32) or an isostructural phase of $BiMn_2O_5$ in sample 5). Thus, it is seen that the activity of bismuth increases significantly when doping with a third element, it "leaves" the crystalline structure of ceria forming an oxide (possibly also in a melt), which in turn forms more complex structures. Thus, the sintering temperature was 750°C. The XRD pattern of ceramics indicates that the phase of the solid solution remained (not shown). The relative density of the ceramic obtained at this temperature calculated as the ratio of densities determined by hydrostatic weighing and by XRD data on the basis of cell parameters was more than 82%, for the system with the addition of zirconium was maximum of 86%, and after sintering at 1000°C it reached 95%, apparently, this increase is due to the fact that bismuth oxide already acts as a sintering additive.

The electrical properties of triple-doped ceria solid electrolytes were analyzed by impedance spectroscopy. Fig. 2 shows the temperature dependencies of the total conductivity of systems in Arrhenius coordinates. It has a thermal activation pattern and can be described by the Arrhenius-Frenkel equation: $\sigma T = A \exp(-E_a/kT)$. With increasing temperature, the oxide ion mobility increased too, so the

Table 1. Main characteristics of $Gd_{0.05}Bi_{0.15}M_{0.05}Ce_{0.75}O_2$ (M = Cu, Zr, Ni, Co, Mn) powders.

No	Sample	d_{XRD}, m	Lattice parameter, Å
0 [10]	$Gd_{0.05}Bi_{0.15}Ce_{0.8}O_2$	8	5.419
1	$Gd_{0.05}Bi_{0.15}Cu_{0.05}Ce_{0.75}O_2$	11	5.427
2	$Gd_{0.05}Bi_{0.15}Zr_{0.05}Ce_{0.75}O_2$	11	5.415
3	$Gd_{0.05}Bi_{0.15}Ni_{0.05}Ce_{0.75}O_2$	10	5.428
4	$Gd_{0.05}Bi_{0.15}Co_{0.05}Ce_{0.75}O_2$	12	5.428
5	$Gd_{0.05}Bi_{0.15}Mn_{0.05}Ce_{0.75}O_2$	8	5.422
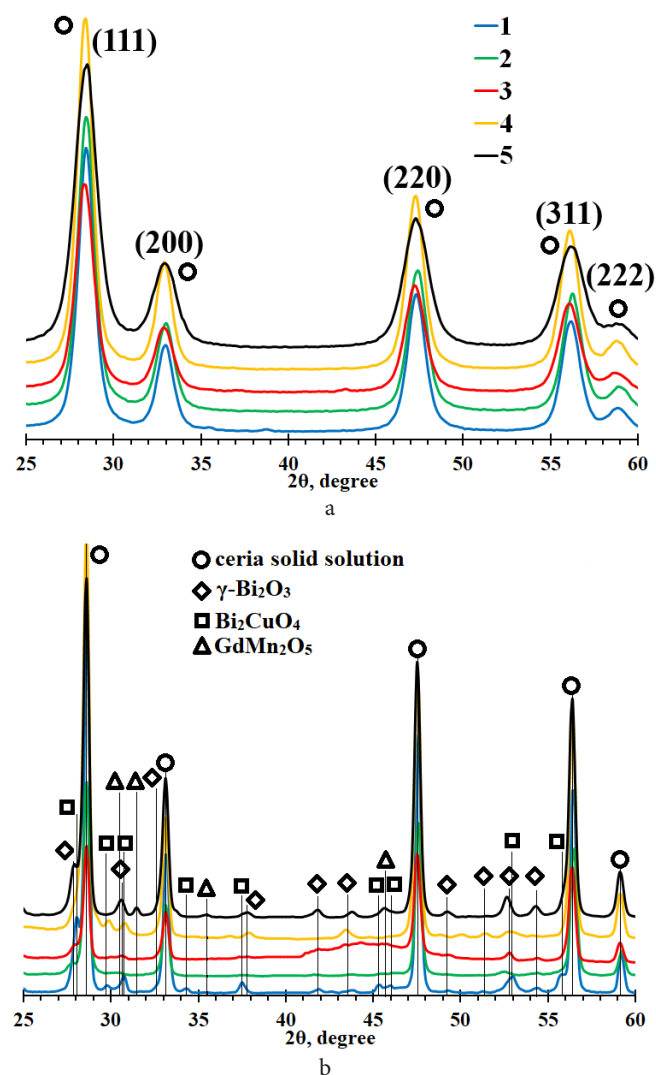
Fig. 1. (Color online) XRD patterns of powders calcined at 500°C (a) and at 1000°C (b).

conductivity increased accordingly. The highest conductivity for intermediate temperature application ($\sigma_{600°C}$ = 8·10^{-3} S/cm) was found in system $Gd_{0.05}Bi_{0.15}Mn_{0.05}Ce_{0.75}O_2$.

The calculated activation energies (E_a, eV) for the samples were: 1 — 0.98, 2 — 1.33, 3 — 1.00, 4 — 1.29, 5 — 0.83. The minimum value of activation energy for the sample 5 may be due to the interaction between concentrated oxygen vacancies and dopant cations in the lattice [15]. The increase in the concentration of mobile ions (oxygen vacancies) leads to the enhanced ionic conductivity of doped ceria. The decreased mobile oxygen vacancies lead to decrease in the
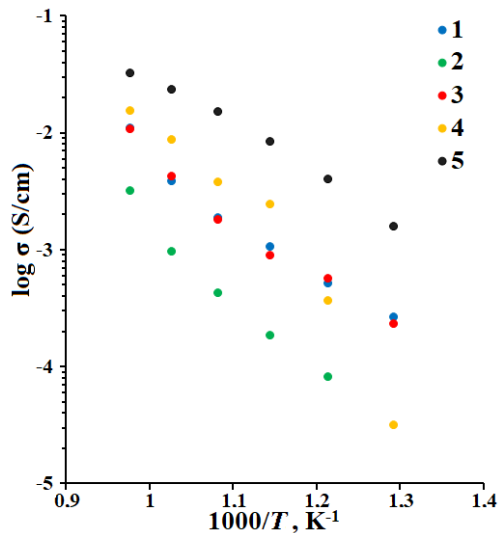
Fig. 2. (Color online) The electrical conductivity of ceramics as a function of temperature.

total ionic conductivity due to the formation of local defects in the ceria structure, i. e. at higher dopant concentrations, the increased probability of dopant clusters lead to formation of deep traps that accommodate the oxygen vacancies and restrict the diffusion of oxygen vacancies [16]. The highest ionic conductivity is achieved when the sample possesses both the lowest activation energy of conduction and the highest pre-exponential term. It is well known that the ionic conduction in doped ceria occurs due to the migration of oxygen ion by the vacancy mechanism, and is mainly determined by Coulombic interactions between defects having opposite charges: positively charged oxygen vacancies and negatively charged dopant. These associations of defects dissociate with the increase in temperature, releasing mobile charge carriers. An increase in the total conductivity in systems with some additives was observed [17–19], in which the effect is associated with the appearance of p-type electron transport, whose fraction in the total conductivity increases with temperature. In order to prepare a dense ceria based electrolyte at a reduced sintering temperature, the addition of low melting-point sintering aids using transition metal oxides such as CoO, CuO, MnO_x, Fe_2O_3, Bi_2O_3, Cr_2O_3, NiO and others. It was shown that the introduction of these additives in the amount of 1–5 mol.% significantly increases the rate of shrinkage and allows reducing the sintering temperature. This densification could be ascribed to the formation of a new binary/ternary/quaternary liquid phase in the grain boundaries of the sample, which resulted in quick densification due to the liquid phase diffusion under capillary action along with grain rearrangement during sintering [20]. In addition, it was recently shown that the nature of manganese species in ceria may vary with the method of synthesis [21]. Moreover, after sintering Mn ions may be in solid solution with ceria, or as a segregated phase along the grains boundaries, or even on the surface of grains, therefore, the sintering mechanism of this system is a very complex phenomenon and requires further experiments.

These results demonstrate that co-doping can improve the conductivity of ceria based electrolytes. When compared with other electrolytes, sintered even at a higher temperature, the electrical conductivity of the developed systems is comparable or higher than the samples doped by REE [16, 22–26] at 600°C. The impedance of the sintered sample at temperature 600°C is shown in Fig. 3. One impedance semicircle is observed, where a low-frequency semicircle is attributed to the electrode polarization resistivity and can include Warburg impedance due to the presence of diffusion processes of the reagent (oxygen) in the near-electrode layer of the electrolyte. In the case of electrodes on which some reversible Faraday process can occur in the presence of diffusion, the impedance and the equivalent circuit look like our scheme. In the temperature range of measurements, the impedance diagrams show similar features and the electrode resistance decreases with the temperature increase.

The Vickers hardness of the polished samples was measured at room temperature by a Struers hardness tester. The hardness was determined by the ratio of the applied load via a geometrically defined indenter to the contact area of the resulting impression using the relation:

$$HV = 1.854 F/d^2,$$

where HV is the Vickers hardness, F is the applied load and d is the indentation diagonal length (arithmetic mean of the two diagonals). In a typical indentation test, the load varied from 0.98 N to 9.8 N. The indentation time was 10 s. Six indentations were made for each load on all the samples. The hardness gradually increased with respect to the applied load. The highest average microhardness of about 10–11 GPa was obtained for the samples $Gd_{0.05}Bi_{0.15}Zr_{0.05}Ce_{0.75}O_2$ (with a microstructure in Fig. 4), for other systems the index was about 8 GPa (with a microstructure in Fig. 5). Although the system with Zr did not have the highest electrical conductivity, they turned out to be the hardest.
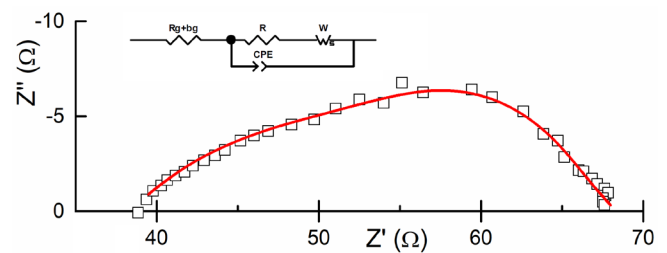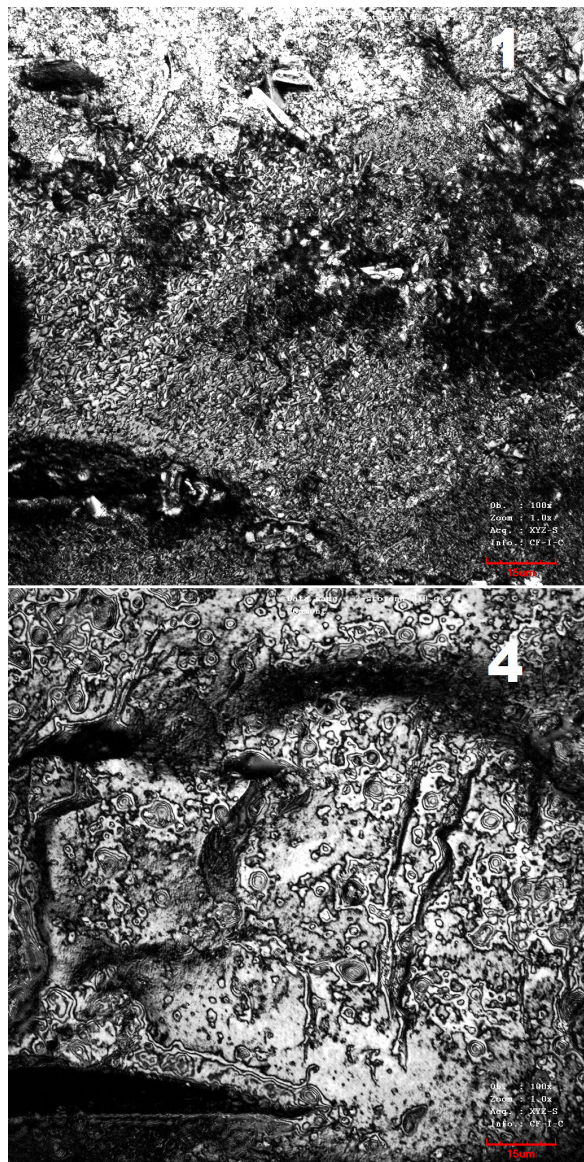

Fig. 3. Impedance spectrum of sample 5 at 600°C in air.
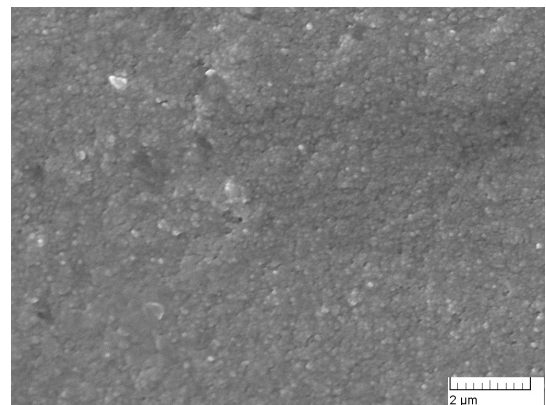
Fig. 4. SEM micrograph of ceramics 2.

Fig. 5. Micrographs of ceramics 1 and 4 (scale bar 15 μm, confocal mode).

4. Conclusions

The effect of the addition of a third dopant (Co, Cu, Ni, Mn, and Zr) on the stability and electrical properties of the solid electrolyte $Gd_{0.05}Bi_{0.15}M_{0.05}Ce_{0.75}O_2$ was investigated. The highest conductivity for an intermediate temperature application ($\sigma_{600°C} = 8\cdot10^{-3}$ S/cm) was found in the system of $Gd_{0.05}Bi_{0.15}Mn_{0.05}Ce_{0.75}O_2$. In particular, it was previously shown that the sintering additive like Mn in GDC leads to a decrease in conductivity, mainly its grain-boundary component due to the contamination of the grain boundaries of ceramics, which did not occur in this work due to the fact that manganese enters into the ceria lattice, without segregating at the grain boundaries as a separate oxide. Nonlinear dependence in systems with Cu, Co, and Ni is apparently due to the appearance of p-type electron transport.

References

1. J. W. Fergus. J. Power Sources. 162, 30 (2006). Crossref
2. D. J. L. Brett, A. Atkinson, N. P. Brandon, S. J. Skinnerd. Chem. Soc. Rev. 37, 1568 (2008). Crossref
3. B. C. H. Steele. Solid State Ionics. 129, 95 (2000). Crossref
4. C. Kleinlogel, L. J. Gauckler. Adv. Mater. 13, 1081 (2001). Crossref
5. A. V. Nikonov, A. V. Spirin, V. R. Khrustov, S. N. Paranin, N. B. Pavzderin, K. A. Kuterbekov, T. N. Nurakhmetov, Y. K. Atazhan. Inorg. Mater. 52, 708 (2016). Crossref
6. V. Gil, C. Moure, P. Durán, J. Tartaj. Solid State Ionics. 178, 359 (2007). Crossref
7. L. Guan, S. Le, S. He, X. Zhu, T. Liu, K. Sun. Electrochim. Acta. 161, 129 (2015). Crossref
8. Y.-P. Fu, C.-W. Tseng, P.-C. Peng. J. Eur. Ceram. Soc. 28, 85 (2008). Crossref
9. G. Accardo, D. Frattini, H. C. Ham, J. H. Han, S. P. Yoon. Ceram. Int. 44, 3800 (2018). Crossref
10. I. V. Zagaynov, S. V. Fedorov, A. A. Konovalov, O. S. Antonova. Mater. Lett. 203, 9 (2017). Crossref
11. A. V. Coles-Aldridge, R. T. Baker. Solid State Ionics. 316, 9 (2018). Crossref
12. K. Venkataramana, C. Madhuri, J. Shanker, Ch. Madhusudan, C. V. Reddy. Ionics. 24, 3075 (2018). Crossref
13. S. A. Muhammed Ali, M. Anwar, A. M. Abdalla, M. R. Somalu, A. Muchtar. Ceram. Int. 43, 1265 (2017). Crossref
14. M. Prekajski, M. Stojmenović, A. Radojković, G. Branković, H. Oraon, R. Subasri, B. Matović. J. Alloy. Compd. 617, 563 (2014). Crossref
15. S. Ramesh, V. P. Kumar, P. Kistaiah, C. V. Reddy. Solid State Ionics. 181, 86 (2010). Crossref
16. K. Venkataramana, C. Madhuri, Y. S. Reddy, G. Bhikshamaiah, C. V. Reddy. J. Alloy Compd. 719, 97 (2017). Crossref
17. D. P. Fagg, V. V. Kharton, J. R. Frade. J. Electroceram. 9, 199 (2002). Crossref
18. E. Yu. Pikalova, A. N. Demina, A. K. Demin, A. A. Murashkina, V. E. Sopernikov, N. O. Esina. Inorg. Mater. 43, 735 (2007). Crossref
19. W. Zajac, L. Suescun, K. Swierczek, J. Molenda. J. Power Sources. 194, 2 (2009). Crossref
20. J. Mackenzie, R. Shuttleworth. Proc. Phys. Soc. 62, 833 (1949). Crossref
21. B. Murugan, A. V. Ramaswamy, D. Srinivas, C. S. Gopinath, V. Ramaswamy. Chem. Mater. 17, 3982 (2005). Crossref
22. A. Arabaci. Metall. Mater. Trans. A Phys. Metall. Mater. Sci. 48, 2282 (2017). Crossref
23. T. H. Santos, J. P. F. Grilo, F. J. A. Loureiro, D. P. Fagg, F. C. Fonseca, D. A. Macedo. Ceram. Int. 44, 1745 (2018). Crossref
24. L. Xiaomin, L. Qiuyue, Z. Lili, L. Xiaomei. J. Rare Earths. 33, 411 (2015). Crossref
25. Z. Tao, H. Ding, X. Chen, G. Hou, Q. Zhang, M. Tang, W. Gu. J. Alloy Compd. 663, 750 (2016). Crossref
26. K. C. Anjaneya, M. P. Singh. J. Alloy Compd. 695, 871 (2017). Crossref